

Poly(3-Hydroxybutyrate-co-3-Hydroxyvalerate)/Purified Cellulose Fiber Composites by Melt Blending: Characterization and Degradation in Composting Conditions

Estefanía Lidón Sánchez-Safont¹, Jennifer González-Ausejo¹, José Gámez-Pérez¹, José María Lagarón², and Luis Cabedo^{1*}

¹Polymers and Advanced Materials Group (PIMA), Jaume I University, 12071 Castelló de la Plana, Spain

²Novel Materials and Nanotechnology Group, IATA, CSIC, Calle Agustín Escardino, 7 Paterna, Valencia, Valencia 46980 Spain

Received November 06, 2015; Accepted December 30, 2015

ABSTRACT: Novel biodegradable composites based on poly(3-hydroxybutyrate-co-3-hydroxyvalerate) (PHBV) and different contents of purified alpha-cellulose fibers (3, 10, 25 and 45%) were prepared by melt blending and characterized. The composites were characterized by scanning electron microscopy (SEM), wide-angle X-ray scattering (WAXS) experiments, thermogravimetric analysis (TGA), differential scanning calorimetry (DSC), dynamic mechanic analysis (DMA) and Shore D hardness measurements. Disintegrability under composting conditions was studied according to the ISO 20200 standard. Morphological results showed that high dispersion of the fibers was achieved during mixing. Good adhesion on the fiber-matrix interface was also detected by SEM. The addition of low and medium cellulose contents did not result in lower thermal resistance with respect to the neat PHBV. A reinforcing effect of the cellulose fibers was detected in all samples, this effect being more pronounced at high temperatures. The composting results show that the addition of the fibers did not affect the disintegrability of the PHBV, and thus compostable “green” low-cost PHBV/cellulose composites can be obtained.

KEYWORDS: PHBV, cellulose, composites, biodegradation, ISO 20200

1 INTRODUCTION

Plastic packaging residues are one of the most serious problems in the management of municipal solid waste since they are mostly resistant to microbial degradation and remain semipermanently in landfills, with the environmental impact that this implies [1, 2]. Composting of biodegradable plastic packaging seems to be one of the most promising solutions for waste management, given the difficulty of separating the organic fraction of municipal waste [2]. Hence, in recent decades there has been a growing interest in the development of biodegradable bioplastics from renewable sources to replace conventional petroleum-based plastics for use in almost all productive sectors, especially in the packaging and agricultural sectors [3, 4].

Among the commercially available biopolymers, biopolyesters have emerged as an alternative to

commodities because of the combination of an easy processability in conventional equipment and good mechanical properties with the ability to biodegrade. Poly(lactic acid) (PLA) is the most widely known and frequently used biopolyester. However, some properties of PLA, such as thermal stability and impact resistance, are lower than those of the commodity polymers used for thermoplastic applications [5]. The low thermal resistance of PLA is a consequence of both a high glass transition temperature (around 70 °C) and a slow crystallization rate, especially at high molecular weights [6, 7]. As a result, many processed products are amorphous and undergo changes in shape at temperatures above 55 °C, which makes PLA inappropriate for use in applications at relatively high temperatures.

Poly(hydroxybutyrate-co-hydroxyvalerate) (PHBV), a bacterial copolyester from the polyhydroxyalkanoate family (PHA), has gained a lot of attention, especially in the packaging field, because of its renewable and non-food competitive origin, biodegradability and performance close to that of some commodity polymers [8, 9]. Although the mechanical performance is similar to that of polypropylene (PP) [10, 11], the gas barrier

*Corresponding author: lcabedo@uji.es

properties to oxygen and aroma are close to those of the polyethylene terephthalate (PET) [12]. In contrast to PLA, PHBV presents a low glass transition temperature and a high degree of crystallinity (with a melting point above 160 °C), and therefore it is suitable for high temperature applications. Nevertheless, PHBV experiments show inferior mechanical performance at temperatures above 80 °C and its high price handicaps its use in low-cost applications [13].

A possible way to reduce the price of PHBV, as well as increase its mechanical performance at high temperatures, is the addition of a second reinforcing phase to develop composite materials. It is well known that the dispersion of fibrillated microparticles or nanoparticles in a polymeric matrix improves the mechanical properties; also, the addition of cheaper loading in high proportions allows reduction in the product's final cost. In this context, the effect of the addition of inorganic fibers to biopolyester matrices on its mechanical, thermic and barrier properties has been widely studied [14, 15].

Within the current context of renewable raw materials, the scientific community has focused its interest on the use of natural fibers as a reinforcing agent for polymer composites because of its advantages in comparison with conventional synthetic or inorganic fillers [16, 17]. In this regard, some of the advantages of natural fibers compared with conventional reinforcing materials are their low cost, low density, high hardness, good thermal properties, acceptable specific strength properties, good availability and biodegradability [18, 19]. In addition, the usage of natural fibers as fillers in polymer composites would allow the use of byproducts or residues from the agricultural and agroalimentary industry. Thus, natural fibers, such as cellulose and its derivatives, which are natural occurring biodegradable fillers, may exert a reinforcement effect on the PHBV matrix as well as reduce the final cost without compromising biodegradability [20].

In the present study, purified alpha-cellulose refined from wood-pulp manufacture was used, where lignin and hemicellulose, which degrade at lower temperatures than cellulose, are removed from the fibers. The advantages of using pure cellulose fibers as compared to unmodified plant fibers include:

1. the possibility of processing at higher temperatures,
2. a higher grade of homogeneity in molar mass and other characteristic properties of the material,
3. higher strength than untreated natural fiber,
4. smaller fiber size,
5. high crystallinity levels which may help to promote higher barrier properties in composites.

Several studies have been carried out in the literature using cellulose fibers with a lignocellulosic nature, but fewer have been conducted using highly purified alpha-cellulose fibers [21–23].

Some studies related to the incorporation of natural lignocellulosic and cellulosic fibers in biopolyesters have been reported [24, 25]. Avella *et al.* reinforced PHBV with heat exploded wheat straw and hemp fibers [26]; Battezzore *et al.* added cellulose derived from rice husk to poly(lactic acid) (PLA) matrices, finding an improvement in mechanical properties [27].

Assessment of the biodegradation of PHAs and PHBV in composting conditions and other environments have been investigated by several authors [8, 28–33]. However, to our knowledge, the biodegradation behavior of composites of PHBV (3% HV)/cellulose fibers obtained by melt blending according to the ISO 20200 standard [34] has not been reported yet.

Within this context, the purpose of this work is to obtain “green,” low-cost composites from commercial PHBV and purified cellulose fibers using the melt blending technique. These composites must contain the highest possible amount of cellulose, increasing mechanical performance (particularly at high temperatures), while retaining their processability and thermal properties, and must be degradable under standard lab-scale composting conditions (ISO 20200 standard).

2 EXPERIMENTAL

2.1 Materials

Poly(3-hydroxybutyrate-co-3-hydroxyvalerate) (PHBV) containing 3 mol% of hydroxyvalerate was supplied by Tianan Biological Materials Co. (Ningbo, P. R. China) in pellet form (ENMATTM Y1000P). A purified alpha-cellulose fiber grade (also referred to as cellulose) (TC90) from CreaFill Fibers Corp. (US) was used. According to the manufacturer's specifications, these fibers have an average fiber length of 60 µm and an average fiber width up to 20 µm. The alpha-cellulose content is > 99.5%.

2.2 PHBV/Cellulose Composite Preparation

PHBV and cellulose fibers were dried at 80 °C for two hours under vacuum before blending to remove moisture. PHBV/cellulose composites with 0, 3, 10, 25 and 45 wt% fiber contents were obtained by melt blending with a ThermoHaake Rheomix Polylab internal mixer for six minutes at 180 °C and a rotor speed of 100 rpm. In order to reduce thermal degradation during blending, the melt temperature was never allowed to reach

190 °C. Each batch was then extracted from the mixing chamber manually and allowed to cool to room temperature in air. Materials generated in the mixing process were then hot pressed at 185 °C and 3 bar for three minutes to produce plates of 0.8 and films of 0.2 mm nominal thickness. All the samples were stored in a vacuum desiccator at room temperature. The samples were named according to the following code: PHBV-XC where X corresponds to the wt% cellulose fiber content.

2.3 Disintegration in Composting Conditions

Biodegradation of PHBV/cellulose composites was evaluated by measuring the disintegrability of the composite plate samples under lab-scale composting conditions. Disintegration tests were carried out according to the ISO 20200 standard [34]. Solid synthetic waste was prepared by mixing 10% of activated mature compost (VIGORHUMUS H-00, purchased from Burás Profesional, S.A., Girona, Spain), 40% sawdust, 30% rabbit feed, 10% corn starch, 5% sugar, 4% corn seed oil and 1% urea. The water content of the mixture was adjusted to 55%. Composite samples were cut from hot pressed plates (15 × 15 × 0.2 mm³) and buried in compost bioreactors at 4–6 cm depth. The samples were placed inside iron mesh bags to simplify their extraction and allow the contact of the compost with the specimens. Bioreactors were incubated at 58 °C. The aerobic conditions were guaranteed by mixing the synthetic waste periodically and adding water according to the standard requirements. Three replicates of each sample were removed from the boxes at different composting times for analysis. Samples were washed with water and dried under vacuum at 40 °C until a constant mass. The disintegration degree was calculated by normalizing the sample weight to the initial weight with Equation 1 [35]:

$$D = \frac{m_i - m_f}{m_i} \times 100 \quad (1)$$

where m_i is the initial dry mass of the test material and m_f is the dry mass of the test material recovered at different incubation stages. The disintegration study was completed by SEM and photographs of samples were taken for visual evaluation.

2.4 Characterization Techniques

Morphology of PHBV/cellulose composites was examined by scanning electron microscopy (SEM) with a JEOL 7001F. The samples were prepared by

cryofracturing after immersion in liquid nitrogen for a few minutes. The surface morphology of composites at different composting times was also investigated by SEM. All the samples were previously coated by sputtering with a thin layer of Pt.

Wide angle X-ray scattering experiments (WAXS) were performed with a Bruker AXS D4 Endeavor diffractometer. Radial scans of intensity versus scattering angle (2θ) were recorded at room temperature in the range of 2 to 30° (step size = 0.02° (2θ), scanning rate = 8 s/step) with identical instrument settings provided by filtered CuK_α radiation ($\lambda = 1.54 \text{ \AA}$), an operating voltage of 40kV, and a filament current of 40 mA.

Thermogravimetric analysis (TGA) was performed with a TG-STD A Mettler Toledo model TGA/STD A851e/LF/1600 to determine the thermal stability of the PHBV/cellulose composites. The samples with an initial weight typically of about 4 mg were heated from 50 °C to 600 °C with a heating rate of 10 °C/min under nitrogen atmosphere. Main thermal parameters were determined from TGA curves, such as the initial decomposition temperature ($T_{5\%}$, temperature at 5% weight loss) and maximum decomposition rate temperature (T_d).

Differential scanning calorimetry (DSC) of PHBV/cellulose composites was conducted on a PerkinElmer DSC 7 thermal analyzer with Ar as the purging gas. The calibration of the DSC was performed with an indium standard sample. Material samples weighing about 6 to 8 mg were heated to 185 °C at 40 °C/min and kept for 3 min to erase thermal history, followed by cooling to room temperature and heating to 185 °C at 10 °C/min. Melting temperatures (T_m) and enthalpies (ΔH_m), as well as crystallization temperatures (T_c) and enthalpies (ΔH_c), were calculated from the corresponding heating/cooling curves. The crystallinity degree (X_c) of the PHBV phase of composites was determined by applying the following expression [36]:

$$X_c(\%) = \frac{\Delta H_m}{w \cdot \Delta H_m^0} \times 100 \quad (2)$$

where ΔH_m (J/g) is the melting enthalpy of the polymer matrix, ΔH_m^0 is the melting enthalpy of 100% crystalline PHBV (perfect crystal) (146 J/g) [37] and w is the polymer weight fraction of PHBV in the blend.

Dynamic mechanic analysis (DMA) experiments were conducted on hot pressed sample platelets (10 × 5 × 0.8 mm) in a PerkinElmer DMA7e. Samples were heated from -20 °C to melting temperature with a heating rate of 5 °C/min at a constant frequency of 1 Hz in the three-point bending mode under Ar flow.

The hardness of PHBV and PHBV/cellulose composites was measured with a Shore D hardness tester Zwick 3100 Shore D (Zwick GmbH, Germany).



3 RESULTS AND DISCUSSION

3.1 Characterization of the PHBV/Cellulose Composites

3.1.1 SEM

Morphological characterization of the cellulose fibers as received and within the composites used in this work was performed with SEM (Figure 1).

Figures 1a and 1b show SEM micrographs of the cellulose fibers at different magnifications. These fibers present a rod-shaped morphology with varying lengths up to 200 μm . In all cases, the diameter is contained within the 10–20 μm range. The broken fibers in Figure 1a and 1b are formed from a bundle of smaller fibrils [23].

The PHBV/cellulose composite SEM micrographs shown in Figure 1c and 1d were obtained from the cryo-fractured surface of the composites with the lowest (3%) and the highest (45%) fiber content, respectively. The examination of the images reveals that a homogeneous dispersion of filler has been achieved. Indeed, no pull-out effect is observed, thus indicating a strong adhesion between the cellulose fibers and the polymer matrix. Broken fibers can be seen on the fractured surface. The good interaction between the cellulose fibers and the polyester matrix can be explained by the formation of a hydrogen-bonding-type interaction between carbonyl groups of PHBV and hydroxyl groups of the cellulose [38]. The morphology observed in the 3 wt% and 45 wt% samples is representative of all the compositions in the studied range.

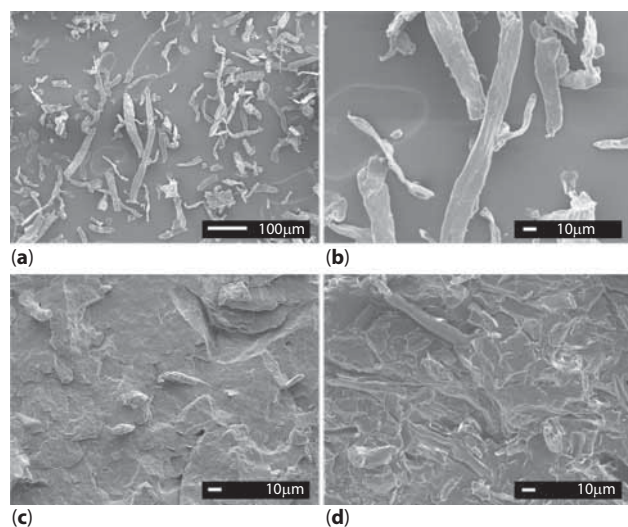


Figure 1 SEM micrographs of cellulose fibers and PHBV/cellulose composites: (a) cellulose low magnification (150x), (b) cellulose high magnification (550x), (c) PHBV-3C (500x) and (d) PHBV-45C (500x).

3.1.2 WAXS

X-ray scattering (WAXS) experiments were conducted on the cellulose powder, the neat PHBV and all the composites studied. The X-ray patterns of the samples are shown in Figure 2.

Three characteristic peaks of PHBV were detected in both PHBV and PHBV/cellulose samples at 2θ angles of 13.4°, 16.9° and 21.5°, corresponding to the (0 2 0), (1 1 0) and (1 0 1) lattice planes of the orthorhombic unit cell of PHBV [36, 39]. The most intense peak at $2\theta = 26$ corresponds to the (002) reflection of the boron nitride, which is present as a nucleating agent in the commercial grade used in this work. There were no changes in the diffraction peak positions of PHBV regardless of the fiber content. This suggests that the crystalline structure of PHBV does not change with the addition of cellulose. The decrease in intensity of the peaks can be explained by a dilution effect as the cellulose content is increased.

3.1.3 DSC

Differential scanning calorimetry (DSC) measurements of PHBV/cellulose composites were performed in order to study the crystallization behavior of these materials. DSC curves of cooling and heating scans, after removal of the thermal history, are displayed in Figure 3. From these curves the characteristic temperatures, enthalpies and crystallinity degree (X_c) of the blends were determined. Results are summarized in Table 1.

PHBV shows an endothermic peak related to its melting point at 168.7 °C and one exothermic peak at 116.4 °C corresponding to crystallization. Pure PHBV presents a crystallinity degree X_c of 67%. This

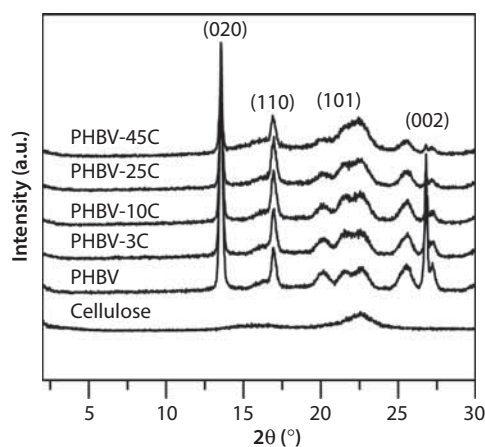


Figure 2 WAXS patterns of the cellulose, the neat PHBV and the PHBV/cellulose composites with 3, 10, 25 and 45 wt% of cellulose.

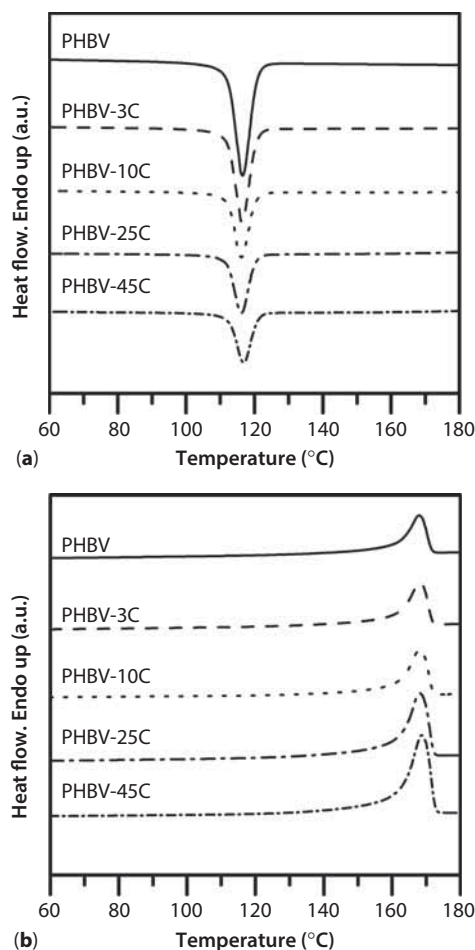


Figure 3 DSC thermograms of: (a) the cooling scan and (b) the heating scan and of the neat PHBV and the PHBV/cellulose composites containing 3, 10, 25 and 45 wt% of cellulose.

Table 1 Crystallization and melting parameters obtained by DSC of neat PHBV and PHBV/cellulose composites.

	T_c (°C)	ΔH_c (J/g)	T_m (°C)	ΔH_m (J/g)	X_c (%)
PHBV	116.4	-87,9	168,7	97,9	67
PHBV-3C	116.4	-87,5	168,0	95,3	67
PHBV-10C	116.1	-83,9	168,2	91,6	70
PHBV-25C	116.1	-70,0	168,2	73,7	67
PHBV-45C	116.9	-63,0	168,0	55,5	69

crystallinity degree is quite high because the PHBV used was a commercial grade containing boron nitride as a nucleating agent.

When cellulose was added to PHBV, no remarkable changes were found in the melting and crystallization peak positions. Regarding X_c variations, PHBV/cellulose composites did not show significant differences. These results seem to contradict other works based

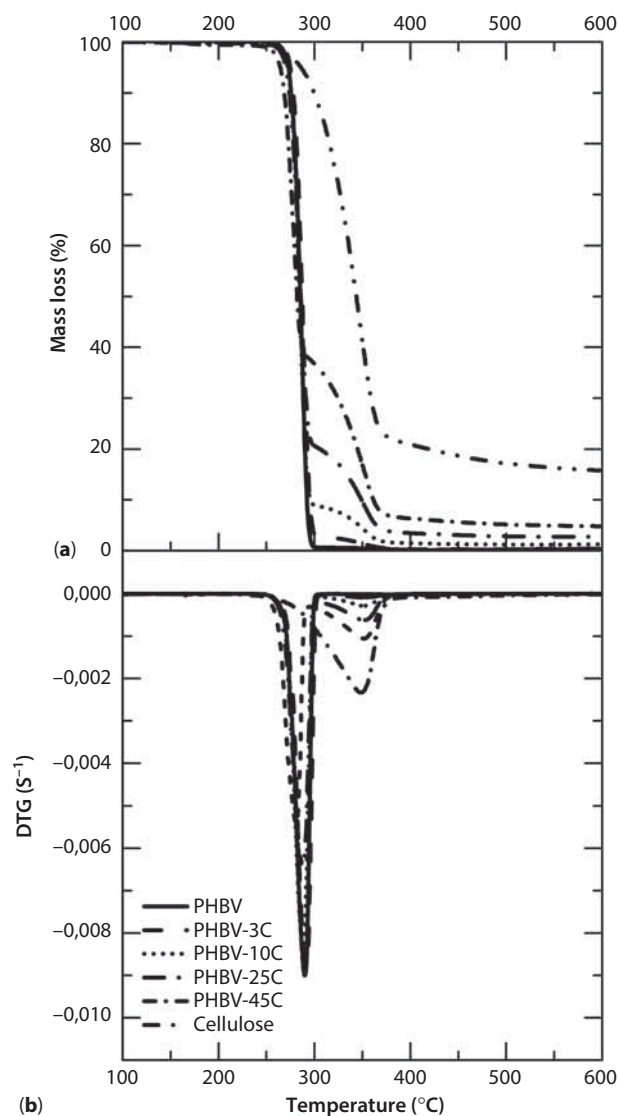


Figure 4 TGA curves of neat PHBV and PHBV/cellulose composites.

on aliphatic polyesters [26, 40], where it has been reported that cellulosic fillers act as nucleating agents and show significant differences in thermal and crystallinity parameters. However, in our case this effect is not appreciable, probably because of the presence of the boron nitride. Therefore, it can be concluded that addition of cellulose fibers barely affects the melting/crystallization behavior of this particular PHBV grade.

3.1.4 TGA

Thermogravimetric analysis (TGA) was conducted to evaluate the thermal degradation of PHBV, cellulose and PHBV/cellulose composites. The TGA curves are shown in Figure 4. The onset degradation temperature ($T_{5\%}$, considered as the temperature at which a

Table 2 Parameters obtained from thermogravimetric analyses of neat PHBV and its composites.

	$T_{5\%}$ (°C)	T_d (°C)	Residue(%) at 600 °C
PHBV	273	290	0.4
PHBV-3C	275	291	0.4
PHBV-10C	272	287	1.3
PHBV-25C	270	288	2.7
PHBV-45C	264	281	4.8
Cellulose	286	348	15.8

5% weight loss occurs), the maximum degradation temperature (T_d , corresponding to the DTG peak) and the residue (%) at 600 °C were determined; results are summarized in Table 2.

Thermogravimetric analysis (TGA) of cellulose revealed that the thermal degradation of these fibers takes place in a single weight loss step around 350 °C, with a residue of 15.8%, in agreement with other works [41].

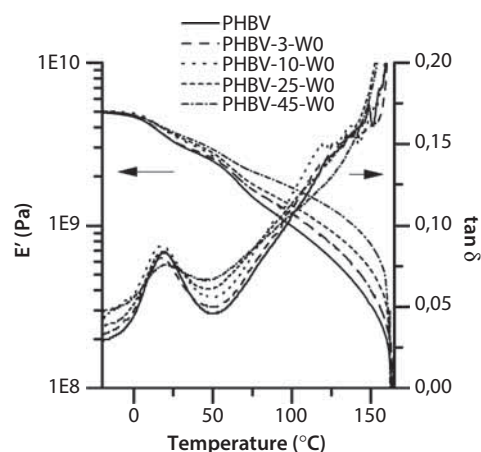
PHBV thermal degradation also takes place in a single weight loss step between 260 °C and 300 °C. This degradation occurs abruptly because of the chain scission reaction mechanism, leading to a dramatic loss of molecular weight and consequently a low thermal stability, as reported in the literature [42]. The onset degradation temperature of PHBV is 273 °C and the maximum decomposition temperature is 290 °C.

In the case of PHBV/cellulose composites, it seems that the addition of low filler contents does not alter the thermal stability of PHBV. The addition of high contents of cellulose fibers, however, slightly decreases the onset degradation temperature and the maximum degradation temperature of the composites. This behavior is attributed to interactions between cellulose and PHBV, similar to those reported by Petinakis *et al.* for PLA starch systems [43].

A secondary degradation peak was found around 350 °C in PHBV/cellulose samples, which was related to cellulose decomposition. The residue at 600 °C was approximately 0.4% and increased with the cellulose addition up to 4.8% for the highest filler content. These residue values are lower than expected on account of the residue of cellulose. The deviation is probably owed to the formation of crotonic acid during the thermal degradation of the PHBV, which is able to hydrolyze cellulose [44], and consequently the residue values are lower.

3.1.5 Mechanical Behavior

Dynamic mechanical analysis (DMA) was performed on PHBV and PHBV/cellulose composites to study

**Figure 5** Storage modulus and Tan- δ curves obtained from the DMA of neat PHBV and its composites.**Table 3** Storage modulus at different temperatures and Shore D hardness of PHBV and PHBV/cellulose composites.

	E' (MPa)		Hardness at 25°C (Shore D)
	25°C	100 °C	
PHBV	3270	998	81±1
PHBV-3C	3310	1170	80±1
PHBV-10C	3560	1170	81±1
PHBV-25C	3630	1320	82±1
PHBV-45C	3740	1700	86±1

the effect of the cellulose content on the mechanical performance throughout the whole temperature range from T_g to melting temperature. The storage modulus (E') and Tan- δ curves are shown in Figure 5, and dependence of the storage modulus on the temperature is summarized in Table 3.

At temperatures below glass transition no major differences in storage modulus were detected among the different materials. Indeed, all the studied samples showed a very stiff behavior. On the other hand, at temperatures above T_g , a rise in the storage modulus was observed as the addition of cellulose increased, therefore showing a good reinforcing effect. This effect can be attributed to the good interaction between the fillers and the biopolyester matrix, according to the SEM observation on the coherent interphase.

At high temperatures, the reinforcement provided by the cellulose fibers was even more noticeable as the matrix decreased its stiffness. In this context, the storage modulus of the pure PHBV at 100 °C dropped to a value ca. 1000 MPa; and that containing 45 wt% of cellulose fibers presented a storage modulus of 1700 MPa, thus showing an increase of 70%. Similar

behavior was reported by Bhardwaj *et al.* [45] for other cellulosic fillers. The increment in the stiffness of the PHBV/cellulose composites at high temperatures improves the performance of this material in applications where temperatures close to or above the boiling point of the water are easily reached (such as food packaging applications).

Tan- δ vs. temperature plots are shown in Figure 5. Tan- δ curves present a single peak at temperatures close to 20 °C, indicating the α -relaxation of the composites, which can be attributed to the glass transition temperatures (T_g). No remarkable differences in T_g values were found for low cellulose contents with respect to the neat PHBV. However, for a 45% cellulose content, Tan- δ peak was slightly shifted towards higher temperatures. This can be attributed to the limitation of chain mobility within the polymer matrix introduced by the fibers [38].

Additionally, Shore D hardness of PHBV and its composites was assessed. Results are summarized in Table 3. From the results it can be concluded that with low filler contents there were no changes in hardness. Nevertheless, the highest loaded composition showed a significant increase of hardness. This increase is in accordance with the reinforcing effect observed in DMA analyses.

3.1.6 Degradation in Composting Conditions of the PHBV/Cellulose Composites

Disintegration in composting conditions was evaluated by measuring the weight loss of PHBV and PHBV/cellulose composite samples according to the ISO 20200 standard. Figure 6 shows the disintegration rate of the samples as a function of time. Weight loss remains practically unchanged until the 20th day of composting.

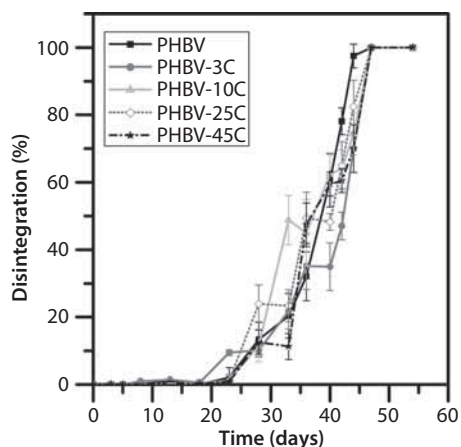


Figure 6 Disintegrability (%) of PHBV and PHBV/cellulose composites under composting conditions as a function of time.

After 20 days the disintegration rate increases markedly to reach total disintegration in 47 days of testing. No significant differences in weight loss rate were observed among samples, so it seems that the cellulose addition does not affect the disintegration rate.

Figure 7 shows the visual appearance of PHBV and PHBV/cellulose composite samples removed from compost at different composting times. No evident changes in the visual examination were detected in the first three weeks of composting, except for a slight surface roughening. This surface roughening indicates the beginning of the disintegration process. In fact, as reported in the literature, the degradation phenomenon occurred with erosion from the surface to the inside [9]. At 42 days clear physical changes on the surface and morphology of the samples were observed. All of the samples were broken into small pieces and showed similar roughening and physical alterations. At longer composting times, samples were more disintegrated, leaving small pieces less than 2 mm in size.

Figure 8 shows an SEM micrograph of the sample PHBV-45C at 40 days under composting conditions where the bacterial growth and the degradation advance can be observed. It can be assumed that the microorganisms attack the polymer amorphous phase in the first stages of the degradation process, following disintegration with assimilation of the crystal structures of the matrix and the filler [46].

4 CONCLUSIONS

In this work, “green,” low-cost PHBV/cellulose composites biodegradable under composting conditions

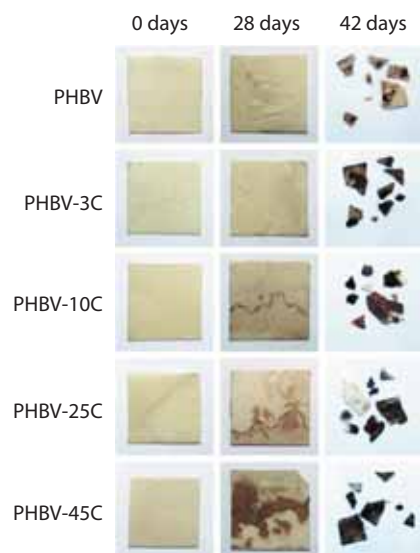


Figure 7 Visual aspect of PHBV and PHBV/cellulose samples after 0, 28 and 42 days under composting conditions.

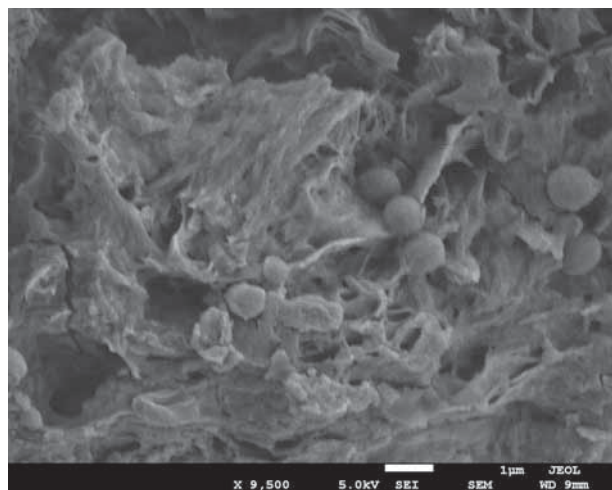


Figure 8 SEM micrograph of the sample with 45% of cellulose content (PHBV-45C) at 40 days of the composting test.

(ISO 20200) were prepared by melt blending with 0, 3, 10, 25 and even 45% cellulose fiber content.

Good adhesion and homogeneous dispersion were obtained in all cases. Composites obtained had a similar thermal stability to that of pure PHBV. Only at 45% cellulose content did a significant decrease in onset degradation temperature ($T_{5\%}$) appear. Cellulose addition did not alter the crystal structure or the crystallinity degree. An increase of the storage modulus as cellulose content rose was noticed. This reinforcing effect was especially pronounced at high temperatures. Indeed, at 100 °C the composite with 45% cellulose content showed an increase of 70% in the storage modulus with respect to neat PHBV. The PHBV/cellulose composites prepared were degradable under composting conditions and the addition of cellulose fibers did not affect the disintegration rate compared with neat PHBV.

ACKNOWLEDGMENTS

Financial support for this research from Ministerio de Economía y Competitividad (project MAT2012-38947-C02-01), Generalitat Valenciana (GV/2014/123), and Pla de Promoció de la Investigació de la Universitat Jaume I (PREDOC/2012/32) is gratefully acknowledged. The authors are also grateful to Raquel Oliver and José Ortega for experimental support.

REFERENCES

1. T. Ishigaki, W. Sugano, A. Nakanishi, M. Tateda, M. Ike, and M. Fujita, The degradability of biodegradable plastics in aerobic and anaerobic waste landfill model reactors. *Chemosphere*. **54**, 225–233 (2004). doi:10.1016/S0045-6535(03)00750-1.

2. G. Kale, T. Kijchavengkul, R. Auras, M. Rubino, S.E. Selke, and S.P. Singh, Compostability of bioplastic packaging materials: An overview. *Macromol. Biosci.* **7**, 255–277 (2007). doi:10.1002/mabi.200600168.
3. J.-W. Rhim, H.-M. Park, and C.-S. Ha, Bio-nanocomposites for food packaging applications. *Prog. Polym. Sci.* **38**, 1629–1652 (2013). doi:10.1016/j.progpolymsci.2013.05.008.
4. D. Briassoulis, An overview on the mechanical behaviour of biodegradable agricultural films. *J. Polym. Environ.* **12**, 65–81 (2004). doi:10.1023/B:JOOE.0000010052.86786.ef.
5. E. Ruiz-Hitzky and F.M. Fernandes, Progress in bio-nanocomposites: From green plastics to biomedical applications. *Prog. Polym. Sci.* **38**, 1391–1772 (2013). doi:10.1016/j.progpolymsci.2013.07.004.
6. L. Nascimento, J. Gamez-Perez, O.O. Santana, J.I. Velasco, M.L. MasPOCH, and E. Franco-Urquiza, Effect of the recycling and annealing on the mechanical and fracture properties of poly(lactic acid). *J. Polym. Environ.* **18**, 654–660 (2010). doi:10.1007/s10924-010-0229-5.
7. J.C. Velazquez-Infante, J. Gamez-Perez, E.A. Franco-Urquiza, O.O. Santana, F. Carrasco, and M. Ll MasPOCH, Effect of the unidirectional drawing on the thermal and mechanical properties of PLA films with different L-isomer content. *J. Appl. Polym. Sci.* **127**, 2661–2669 (2013). doi:10.1002/app.37546.
8. S. Luo and A.N. Netravali, A study of physical and mechanical properties of poly(hydroxybutyrate-co-hydroxyvalerate) during composting. *Polym. Degrad. Stab.* **80**, 59–66 (2003). doi:10.1016/S0141-3910(02)00383-X.
9. Y.-X. Weng, Y. Wang, X.-L. Wang, and Y.-Z. Wang, Biodegradation behavior of PHBV films in a pilot-scale composting condition. *Polym. Test.* **29**, 579–587 (2010). doi:10.1016/j.polymertesting.2010.04.002.
10. S. Pilla, *Handbook of Bioplastics and Biocomposites Engineering Applications*, Scrivener Publishing LLC, Salem, Mass. (2011). doi:10.1002/9781118203699.
11. R. Smith, (Ed.), *Biodegradable Polymers for Industrial Applications*, Elsevier, London (2005). doi:10.1016/B978-1-85573-934-5.50021-0.
12. D. Cava, E. Gimenez, R. Gavara, and J.M. Lagaron, Comparative performance and barrier properties of biodegradable thermoplastics and nano-biocomposites versus PET for food packaging applications. *J. Plast. Film Sheeting.* **22**, 265–274 (2006). doi:10.1177/8756087906071354.
13. J.M. Lagaron and A. Lopez-Rubio, Nanotechnology for bioplastics: Opportunities, challenges and strategies. *Trends Food Sci. Technol.* **22** 611–617 (2011). doi:10.1016/j.tifs.2011.01.007.
14. P. Bordes, E. Pollet, and L. Averous, Nano-biocomposites: Biodegradable polyester/nanoclay systems. *Prog. Polym. Sci.* **34** 125–155 (2009). doi:10.1016/j.progpolymsci.2008.10.002.
15. M.D. Sanchez-Garcia and J.M. Lagaron, Novel clay-based nanobiocomposites of biopolyesters with synergistic barrier to UV light, gas, and vapour. *J. Appl. Polym. Sci.* **118**, 188–199 (2010). doi:10.1002/app.31986.
16. P. Wambua, J. Ivens, and I. Verpoest, Natural fibres: Can they replace glass in fibre reinforced plastics?

- Compos. Sci. Technol.* **63**, 1259–1264 (2003). doi:10.1016/S0266-3538(03)00096-4.
17. J.K. Pandey, S.H. Ahn, C.S. Lee, A.K. Mohanty, and M. Misra, Recent advances in the application of natural fiber based composites. *Macromol. Mater. Eng.* **295** 975–989 (2010). doi:10.1002/mame.201000095.
 18. A.K. Mohanty, M. Misra, and G. Hinrichsen, Biofibres, biodegradable polymers and biocomposites: An overview. *Macromol. Mater. Eng.* **276–277**, 1–24 (2000). doi:10.1002/(SICI)1439-2054(20000301)276:1<1::AID-MAME1>3.0.CO;2-W.
 19. A. López-Rubio, J.M. Lagaron, M. Ankerfors, T. Lindström, D. Nordqvist, A. Mattozzi, et al., Enhanced film forming and film properties of amylopectin using micro-fibrillated cellulose. *Carbohydr. Polym.* **68**, 718–727 (2007). doi:10.1016/j.carbpol.2006.08.008.
 20. G. Bogoeva-Gaceva, M. Avella, M. Malinconico, A. Buzarovska, A. Grozdanov, G. Gentile, et al., Natural fiber eco-composites. *Polym. Compos.* **28** 98–107 (2007). doi:10.1002/pc.20270.
 21. M. Haghghat, A. Zadhoush, and S.N. Khorasani, Physicomechanical properties of α -cellulose-filled styrene-butadiene rubber composites. *J. Appl. Polym. Sci.* **96**, 2203–2211 (2005). doi:10.1002/app.21691.
 22. W. Qiu, T. Endo, and T. Hirotsu, Interfacial interaction, morphology, and tensile properties of a composite of highly crystalline cellulose and maleated polypropylene. *J. Appl. Polym. Sci.* **102**, 3830–3841 (2006). doi:10.1002/app.24846.
 23. A. Fendler, M.P. Villanueva, E. Gimenez, and J.M. Lagarón, Characterization of the barrier properties of composites of HDPE and purified cellulose fibers. *Cellulose.* **14**, 427–438 (2007). doi:10.1007/s10570-007-9136-x.
 24. L. Jiang, J. Huang, J. Qian, F. Chen, J. Zhang, M.P. Wolcott, et al., Study of poly(3-hydroxybutyrate-co-3-hydroxyvalerate) (PHBV)/bamboo pulp fiber composites: Effects of nucleation agent and compatibilizer. *J. Polym. Environ.* **16**, 83–93 (2008). doi:10.1007/s10924-008-0086-7.
 25. R. Krishnaprasad, N.R. Veena, H.J. Maria, R. Rajan, M. Skrifvars, and K. Joseph, Mechanical and thermal properties of bamboo microfibril reinforced polyhydroxybutyrate biocomposites. *J. Polym. Environ.* **17**, 109–114 (2009). doi:10.1007/s10924-009-0127-x.
 26. M. Avella, G. La Rota, E. Martuscelli, M. Raimo, P. Sadocco, G. Elegir, and R. Riva, PHBV and wheat straw fibre composites: Thermal, mechanical properties and biodegradation. *J. Mater. Sci.* **5**, 829–836 (2000).
 27. D. Battagazzore, S. Bocchini, J. Alongi, A. Frache, and F. Marino, Cellulose extracted from rice husk as filler for poly(lactic acid): Preparation and characterization. *Cellulose.* **21**, 1813–1821 (2014). doi:10.1007/s10570-014-0207-5.
 28. K.C. Batista, D.A.K. Silva, L.A.F. Coelho, S.H. Pezzin, and A.P.T. Pezzin, Soil biodegradation of PHBV/peach palm particles biocomposites. *J. Polym. Environ.* **18**, 346–354 (2010). doi:10.1007/s10924-010-0238-4.
 29. S.P.C. Gonçalves, S.M. Martins-Franchetti, and D.L. Chinaglia, Biodegradation of the films of PP, PHBV and its blend in soil. *J. Polym. Environ.* **17**, 280–285 (2009). doi:10.1007/s10924-009-0150-y.
 30. Y.-X. Weng, X.-L. Wang, and Y.-Z. Wang, Biodegradation behavior of PHAs with different chemical structures under controlled composting conditions. *Polym. Test.* **30**, 372–380 (2011). doi:10.1016/j.polymertesting.2011.02.001.
 31. M.T. Gutierrez-Wing, B.E. Stevens, C.S. Theegala, I.I. Negulescu, and K.A. Rusch, Aerobic biodegradation of polyhydroxybutyrate in compost. *Environ. Eng. Sci.* **28**, 477–488 (2011).
 32. S. Wang, C. Song, G. Chen, T. Guo, J. Liu, B. Zhang, et al., Characteristics and biodegradation properties of poly(3-hydroxybutyrate-co-3-hydroxyvalerate)/organophilic montmorillonite (PHBV/OMMT) nanocomposite. *Polym. Degrad. Stab.* **87**, 69–76 (2005). doi:10.1016/j.polyimdegradstab.2004.07.008.
 33. B.-I. Sang, K. Hori, Y. Tanji, and H. Unno, Fungal contribution to in situ biodegradation of poly(3-hydroxybutyrate-co-3-hydroxyvalerate) film in soil. *Appl. Microbiol. Biotechnol.* **58**, 241–247 (2002). doi:10.1007/s00253-001-0884-5.
 34. UNE-EN ISO, UNE-EN ISO 20200 Determinación del grado de desintegración de materiales plásticos bajo condiciones de compostaje simuladas en un laboratorio (2006).
 35. A.V. García, M.R. Santonja, A.B. Sanahuja, and M.C.G. Selva, Characterization and degradation characteristics of poly(ϵ -caprolactone)-based composites reinforced with almond skin residues. *Polym. Degrad. Stab.* **108**, 269–279 (2014). doi:10.1016/j.polyimdegradstab.2014.03.011.
 36. L.N. Carli, J.S. Crespo, and R.S. Mauler, PHBV nanocomposites based on organomodified montmorillonite and halloysite: The effect of clay type on the morphology and thermal and mechanical properties. *Compos. Part A Appl. Sci. Manuf.* **42**, 1601–1608 (2011). doi:10.1016/j.compositesa.2011.07.007.
 37. Y.-M. Corre, S. Bruzard, J.-L. Audic, and Y. Grohens, Morphology and functional properties of commercial polyhydroxyalkanoates: A comprehensive and comparative study. *Polym. Test.* **31**, 226–235 (2012). doi:10.1016/j.polymertesting.2011.11.002.
 38. Y. Srithep, T. Ellingham, J. Peng, R. Sabo, C. Clemons, L.-S. Turng, et al., Melt compounding of poly(3-hydroxybutyrate-co-3-hydroxyvalerate)/nanofibrillated cellulose nanocomposites. *Polym. Degrad. Stab.* **98**, 1439–1449 (2013). doi:10.1016/j.polyimdegradstab.2013.05.006.
 39. J. Li, C. Sun, and X. Zhang, Preparation, thermal properties, and morphology of graft copolymers in reactive blends of PHBV and PPC. *Polym. Compos.* **33**, 1737–1749 (2012). doi:10.1002/pc.
 40. A. Dufresne, D. Dupeyre, and M. Paillet, Lignocellulosic flour-reinforced poly(hydroxybutyrate-co-valerate) composites. *J. Appl. Polym.* **87**, 1302–1315 (2003).
 41. M.D. Sanchez-Garcia and J.M. Lagaron, On the use of plant cellulose nanowhiskers to enhance the barrier properties of polylactic acid. *Cellulose.* **17**, 987–1004 (2010). doi:10.1007/s10570-010-9430-x.

42. Q.-S. Liu, M.-F. Zhu, W.-H. Wu, and Z.-Y. Qin, Reducing the formation of six-membered ring ester during thermal degradation of biodegradable PHBV to enhance its thermal stability. *Polym. Degrad. Stab.* **94**, 18–24 (2009). doi:10.1016/j.polymdegradstab.2008.10.016.
43. E. Petinakis, X. Liu, L. Yu, C. Way, P. Sangwan, K. Dean, *et al.*, Biodegradation and thermal decomposition of poly(lactic acid)-based materials reinforced by hydrophilic fillers. *Polym. Degrad. Stab.* **95**, 1704–1707 (2010). doi:10.1016/j.polymdegradstab.2010.05.027.
44. P. Gatenholm and A. Mathiasson, Biodegradable natural composites. II. Synergistic effects of processing cellulose with PHB. *J. Appl. Polym. Sci.* **51**, 1231–1237 (1994). doi:10.1002/app.1994.070510710.
45. R. Bhardwaj, A.K. Mohanty, L.T. Drzal, F. Pourboghra, and M. Misra, Renewable resource-based green composites from recycled cellulose fiber and poly(3-hydroxybutyrate-co-3-hydroxyvalerate) bioplastic. *Biomacromolecules*. **7**, 2044–2051 (2006).
46. M.P. Arrieta, J. López, E. Rayón, and A. Jiménez, Disintegrability under composting conditions of plasticized PLA–PHB blends. *Polym. Degrad. Stab.* **108**, 307–318 (2014). doi:10.1016/j.polymdegradstab.2014.01.034.